STEWARD-1328

PREPRINTS

of the

STEWARD OBSERVATORY

THE UNIVERSITY OF ARIZONA
TUCSON, ARIZONA 85721 U.S.A.

FERMILAB
APR 26 1996
LIBRARY

Fermilab Library
0 1160 0042484 0

No. 1328

BONDI-HOYLE ACCRETION ONTO Sgr A*

R. F. Coker
Physics Department, The University of Arizona Arizona U.
Tucson, Arizona 85721

F. Melia[1]
Physics and Astronomy Departments, The University of Arizona Arizona U.
Tucson, Arizona 85721

[1]Presidential Young Investigator

Fourth ESO/CTIO Workshop on the Galactic Center,
Ed. Roland Gredel

Arizona Theoretical Astrophysics Preprint #96-8

Bondi-Hoyle Accretion onto Sgr A*

R. F. Coker

Physics Department, University of Arizona, Tucson, AZ 85721

F. Melia[1]

Physics and Astronomy Departments, University of Arizona, Tucson, AZ 85721

1. Introduction

Multi-wavelength observations (Geballe *et al.* 1991) of the inner ~ 0.3 pc region of the Galaxy provide strong evidence for the presence of an ambient Galactic center wind of 3×10^{-3} $M_\odot$ per year flowing near the unique variable, nonthermal point source Sgr A*, which, based on kinematic studies of nearby stars (Haller *et al.* 1996) might have a mass of $\sim 10^6$ $M_\odot$. The conditions suggest that the luminosity and spectrum of Sgr A* may be primarily due to its accreting this $v \sim 700$ km s^{-1} and $n \sim 5.5\times10^3$ cm^{-3} wind (Melia 1992) via the Bondi-Hoyle Process. Bondi-Hoyle accretion and its accompanying bow shock will occur whenever a gas flowing in a potential well has a kinetic energy density smaller than its gravitational potential energy density. In the case of Sgr A*, this condition is met at the accretion radius, $R_{acc} \equiv 2GM/v^2 \sim 5\times10^{16}$ cm $\sim 1/2''$. Using the finite-differencing 3D hydrodynamical (HD) code ZEUS (Stone & Norman 1992), we have carried out basic simulations of this activity in order to determine the temperature, density, and velocity profiles of the resulting flow as well as the mass and angular momentum accreted by Sgr A*. We show that this Bondi-Hoyle accretion, which is responsible for an infall of up to $\sim 10^{22}$ g s^{-1} onto Sgr A*, also produces a downstream, focused flow with a radius and mechanical luminosity that may be the cause of the $\sim 1''$ mini-cavity (and its associated "blobs") in the streamer $3.5''$ to the southwest of Sgr A* (Yusef-Zadeh *et al.* 1989). We show that either a highly concentrated cluster of stellar remnants or a point mass can produce such a collimated flow.

2. The Simulations

Two 3D HD simulations have been carried out, one for a 10^6 $M_\odot$ point mass and the other for an isothermal distribution of 10^6 1 $M_\odot$ stellar remnants. In both cases, the cube of solution is 32 R_{acc} on a side with 115 zones per side in the single point mass case and 75 zones per side in the isothermal distribution run (with higher resolution nearer the central region). The wind is modeled as a Mach 10 planar flow entering the volume of solution from one side through a 0.1 pc

[1] Presidential Young Investigator

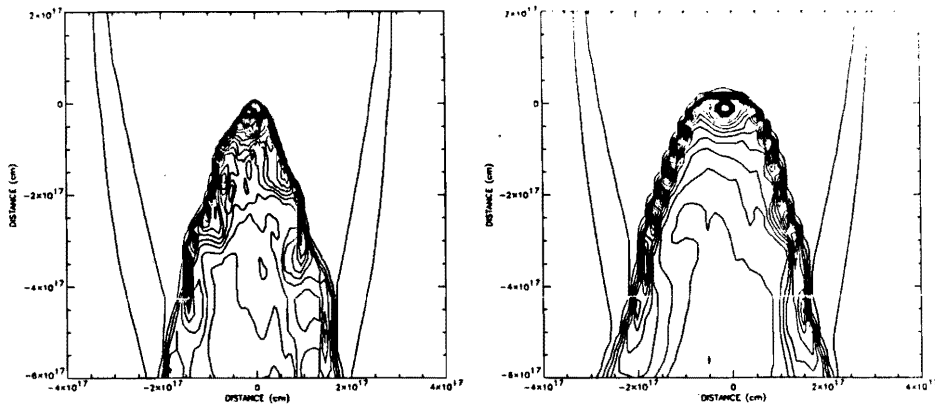

Figure 1. Cross-sectional contour plot of the density ρ in the Bondi-Hoyle bow shock for both runs (the single point mass case on the left and the isothermal distribution on the right). There are 25 contours increasing linearly with ρ from 2.3×10^3 to 5.8×10^4 cm^{-3}. Sgr A* is located at 0,0, and the wind enters from above.

radius circle while the other edges of the cube permit only gas outflow. The code uses van Leer advection and fully explicit time integration, determined by the Courant condition. Although the dissipation of the magnetic field entrained by the highly ionized flow is expected to be an important heating agent (Melia 1992, 1994), it has not as yet been included. Also, bremsstrahlung and, especially, magnetic bremsstrahlung emission become significant toward smaller radii; they too have not yet been included. Instead, the medium is assumed to be an adiabatic polytropic gas. See Stone & Norman (1992) for more details.

The 10^6 $M_\odot$ point mass accretor is modeled as a totally absorbing sphere with a radius of 0.03 R_{acc}; its interior is kept effectively empty by resetting the density in the interior zones to very small values. The mass and specific angular momentum accretion rates are determined by the gas flowing through this inner boundary. The isothermal distribution is truncated at 1 R_{acc} and given a velocity dispersion of 600 km/sec so that the total integrated mass is correctly 10^6 $M_\odot$. Note that if the velocity dispersion is less than $\sim$ 600 km/sec (or, equivalently, the 10^6 1 $M_\odot$ objects have a core radius larger than $R_{acc}/2$), no shock front forms and no Bondi-Hoyle accretion occurs at all.

3. Resulting Profiles

In Figure 1 we show the cross-sectional density contours for the two simulations. The bow shock is clearly evident in both cases, although it is sharper, more focused, and more erratic in the black hole case. The turbulent post-shock flow is evident, as well as the post-shock focusing of the gas into a "tube". Both configurations yield similar profiles and produce a fairly stable shock front at $\sim 1R_{acc}$ while having central densities and temperatures more than 100 times that of the inflowing wind.

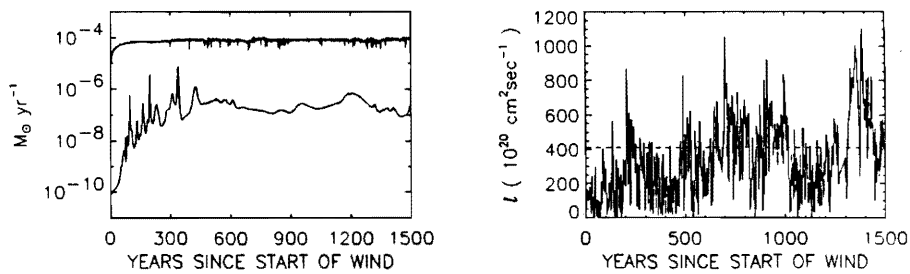

Figure 2. On the left is the mass accretion rate versus time for the two runs; the single point mass case is the thick upper line while the distributed masses case is the thin lower line. Note that equilibrium requires $\sim$ 500 years. On the right is the specific angular momentum accreted by the black hole versus time. The dashed line is the time averaged equilibrium value.

4. Specific Angular Momentum and Mass Accretion Rates

It has long been known that spherical accretion onto a point mass will yield the Hoyle-Lyttleton (1939) accretion rate, $\dot{M}_{HL} \equiv 4\pi(GM)^2\rho_{wind}/v^3$. In the case of Sgr A*, this is $\sim$ 1/30th of the total Galactic wind or $\sim 10^{-4} M_\odot$ yr^{-1}. In Figure 2 we show the resulting total specific angular momenturm and mass accretion rates. $\dot{M}$ for the black hole run agrees with the Hoyle-Lyttleton theory and earlier results (Ruffert & Melia 1994) to within $\sim$25% while the distributed masses accrete less due to the M^2 dependence of $\dot{M}$. However, the latter's time variability is much larger due to the smaller length scales involved. The $\dot{M}$ for the isothermal distribution was calculated assuming that all of the 1 $M_\odot$ objects are local perfect Hoyle-Lyttleton accretors.

The average specific angular momentum accreted by the black hole is 4×10^{22} cm^2 sec^{-1}. This yields a "circularization" radius ($\equiv 2l^2/[c^2 R_g]$ where $R_g \equiv 2GM/c^2$) of $\sim$ 50 R_g $\sim$ 1 A.U. Thus, most of the infalling angular momentum is cancelled in the post shock flow and any resulting accretion disk, in the black hole scenario, is likely, even in the case of highly non-uniform inflow, to have a radius of less than a few A.U. In the case of the distributed masses, the radio flux that is identified with Sgr A* may be coming from hot, magnetized gas trapped in the core of the stellar remnant distribution. If the core radius of the distributed masses is more than $\sim R_{acc}/2$ then the mass accretion rate falls to $\sim 10^{-10}$ $M_\odot$ yr^{-1} and no gas gets trapped within the cluster.

5. Creating the Mini-Cavity

As discussed elsewhere (Melia, Coker & Yusef-Zadeh 1996; Melia 1996), the focused post-shock flow carries mass and mechanical energy flux into the Bar 3.5″ to the southwest of Sgr A*. The radius of this flow ($\sim$1″) closely matches the observed radius of the mini-cavity (Yusef-Zadeh *et al.* 1990), suggesting that

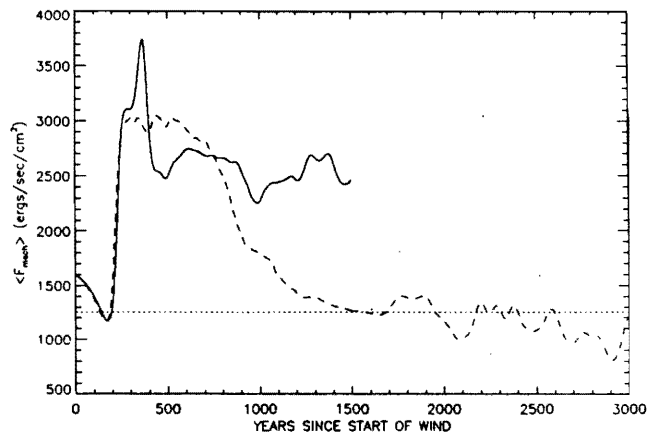

Figure 3. Assuming the mini-cavity has a radius of 1″ and is located 3.5″ behind Sgr A*, these curves show the average mechanical flux for the two runs (solid = black hole; dashed = isothermal distribution; dotted = minimum required to power the mini-cavity).

the mechanical energy brought in by this gas flow is providing the power to sustain the mini-cavity's luminosity of $\approx 6\times10^{37}$ ergs sec^{-1} (Lutz *et al.* 1993). In Figure 3 we show the calculated mechanical flux ($\equiv \rho v^2 v_z/2$) at the location of the mini-cavity. The black hole case clearly has sufficient mechanical energy to power the mini-cavity while the isothermal distribution is marginal due to its less efficient focusing. In addition, the mass transfer rates and variability are consistent with forming the "blobs" connecting Sgr A* and the mini-cavity. However, the inclusion of heating and cooling may change this picture significantly. Thus, in principle, either a $10^6 M_\odot$ black hole or a concentration of 10^6 1 $M_\odot$ stellar remnants (*e.g.*, white dwarfs) within 1 R_{acc} could account for the mini-cavity. Further study is required to determine if the gas trapped by the cluster can account for the observed radio spectrum of Sgr A*.

References

Geballe, T. R., Krisciunas, K., & Bailey, J. A. 1991, ApJ, 370, L73

Haller, J. W., Rieke, M. J., Rieke, G. H., Tamblyn, P., Close, L., & Melia, F. 1996, ApJ, 456, 194

Hoyle, F. & Lyttleton, R. A. 1939, Proc. Cam. Phil. Soc., 35, 405

Lutz, D., Krabbe, A., & Genzel, R. 1993, ApJ, 419, 244

Melia, F. 1992, ApJ, 387, L25

Melia, F. 1994, ApJ, 426, 577

Melia, F. 1996, these proceedings

Melia, F., Coker, R. F., & Yusef-Zadeh, F. 1996, ApJ, 460, L33

Ruffert, M. & Melia, F. 1994, A&A, 288, L29

Stone, J. M., & Norman, M. L. 1992, ApJS, 80, 753

Yusef-Zadeh, F., Morris, M. & Ekers, R. D. 1989, in The Center of the Galaxy, M. Morris, Dordrecht: Kluwer, 443

Yusef-Zadeh, F., Morris, M., & Ekers, R. D. 1990, Nature, 348, 45